

# Estimation of molar absorptivities and pigment sizes for eumelanin and pheomelanin using femtosecond transient absorption spectroscopy

Ivan R. Piletic, Thomas E. Matthews, and Warren S. Warren<sup>a)</sup>*Department of Chemistry, Duke University, Durham, North Carolina 27708-0346, USA*

(Received 7 August 2009; accepted 28 October 2009; published online 13 November 2009)

Fundamental optical and structural properties of melanins are not well understood due to their poor solubility characteristics and the chemical disorder present during biomolecular synthesis. We apply nonlinear transient absorption spectroscopy to quantify molar absorptivities for eumelanin and pheomelanin and thereby get an estimate for their average pigment sizes. We determine that pheomelanin exhibits a larger molar absorptivity at near IR wavelengths (750 nm), which may be extended to shorter wavelengths. Using the molar absorptivities, we estimate that melanin pigments contain  $\sim 46$  and 28 monomer units for eumelanin and pheomelanin, respectively. This is considerably larger than the oligomeric species that have been recently proposed to account for the absorption spectrum of eumelanin and illustrates that larger pigments comprise a significant fraction of the pigment distribution. © 2009 American Institute of Physics. [doi:10.1063/1.3265861]

Melanin is an important biological pigment that naturally occurs in plants and animals. In humans, it is predominantly found in hair, eyes, and skin where it is produced in organelles called melanosomes. It is generally perceived to play a photoprotective role in the skin by nonradiatively downconverting absorbed UV photons to heat.<sup>1</sup> The structural and chemical characteristics of melanins have not been fully elucidated to date. Difficulties in their chemical analyses arise from low solubilities, harsh extraction procedures, and chemical disorder present at the molecular level. Melanins generally come in two polymeric forms: eumelanin (black) and pheomelanin (red/brown).<sup>2</sup> Their biosynthetic pathways involve the oxidation of tyrosine leading to the formation of indoles and benzothiazines (in the presence of cysteine). Figure 1 displays the main precursors that polymerize to form eumelanin and pheomelanin.<sup>3</sup> Unfortunately, the details of the polymerization process are not well understood. Fundamental questions regarding the distribution of monomers, intermolecular bonding patterns, and the average size of the polymer remain unanswered. In this work, we apply optical transient absorption spectroscopy to address the issues of polymer size and molar absorptivity.

Most melanin structural, functional, and computational studies have focused on eumelanin. X-ray scattering and tunneling microscopy experiments have suggested that oligomers of four to six indole species form and may represent a fundamental structural unit of eumelanin termed a “protomolecule”.<sup>4</sup> Alternatively, ultrafiltration studies have been used to isolate larger melanin species ranging in molecular weight from  $<1000$  to  $>10\,000$  amu.<sup>5</sup> Numerous experimental and theoretical efforts have also focused on correlating structure with the characteristic broad absorption spectrum of melanins.<sup>6–8</sup> Initial studies<sup>6</sup> suggested that melanins are extended polymers with a band structure similar to amorphous semiconductors, and this was used to explain

their switching behavior.<sup>9</sup> More recent work introduced a chemical disorder model, where various oligomers with different absorption spectra combine to produce the broad featureless spectrum.<sup>7</sup> The conflicting results and models warrant further study with more sensitive methods.

We employ transient absorption spectroscopy to investigate melanins because it is uniquely poised to examine more of their energy landscape, which may be related to structural parameters as we show below. Recently, the transient absorption spectra of melanins subsequent to UV excitation have been measured illustrating that rapid nonradiative relaxation processes dominate the response.<sup>1,10</sup> In addition, these studies have also revealed the presence of numerous excited state transitions, suggesting that pigment structures possess extended conjugation, which would give rise to a quasiband

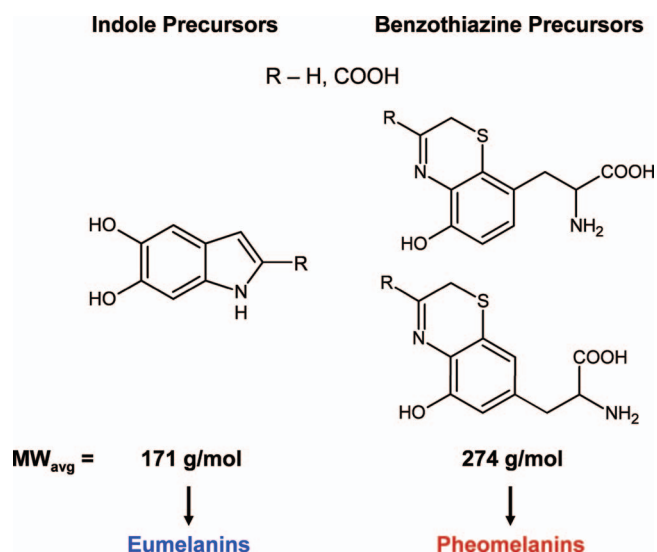


FIG. 1. Monomeric precursors present in the synthesis of eumelanin and pheomelanin. The molar masses of each species were averaged (with equal weighting) in order to determine the average monomer molar masses that were used in subsequent calculations.

<sup>a)</sup>Electronic mail: warren.warren@duke.edu.

energy level structure. Here we apply transient absorption in the near-IR spectral range (750–810 nm) to extract fundamental optical constants from calibrated signal amplitudes that are subsequently related to structural information. The near IR spectral region is of particular interest since it only appears when melanins polymerize because precursors predominantly absorb at UV wavelengths.<sup>11</sup>

In a typical transient absorption experiment, two time delayed femtosecond pulses are used to pump and probe specific energy levels. Molecules that are excited by the pump pulse deplete the ground state in addition to populating an excited state. A subsequent probe pulse may sense the depletion of the ground state and/or stimulated emission from the excited state because of increased sample transmission. Decreased sample transmission at the probe wavelength is a consequence of excited state absorption. The small transmission changes are detected using a modulation transfer technique.<sup>12</sup> Amplitude modulations imposed on the pump pulses will transfer to the probe pulses in the event of ground state depletion, stimulated emission or excited state absorption, which is picked up by a lock-in amplifier. Details of the laser apparatus are provided in the supplementary material.<sup>13</sup> We used two collinear ( $\sim 140$  fs) pulses centered at 810 and 750 nm for pumping and probing melanins, respectively. The average laser power for these experiments was 5 mW (4 mW pump; 1 mW probe) or less. All experimental data reported in this work were obtained on the same day, which prevented variable laser focusing and beam overlap to affect the calibration procedures.

The samples that were used in these experiments consisted of Sepia eumelanin and synthetic pheomelanin, which represent reasonable models for melanins derived from humans. Sepia eumelanin in particular is similar to melanosomes found in human skin because it is granular with aggregated particles that are  $\sim 150$  nm in size containing proteins, metals, and lipids.<sup>14</sup> Differences in particle morphology and composition for Sepia eumelanin and melanosomes are relatively small in comparison with synthetically derived eumelanins (relatively pure and amorphous). Unfortunately, such an abundant natural pheomelanin source is unavailable because it is difficult to extract pheomelanins from hair or other sources. We therefore synthesized pheomelanin according to the optimized procedure given by Ito<sup>15</sup> and obtained a 50% reaction yield. Any residual tyrosinase that was present in the final yield represents  $<8\%$  of the total mass and therefore gives rise to a small error in subsequent molar mass calculations. Sepia eumelanin and synthetic pheomelanin were dissolved in a 50 mM phosphate buffer solution ( $pH=7$ ) at a concentration of 0.84 mg/ml. Filtration methods were used to obtain an optically viable suspension solution for Sepia eumelanin. The filter size ( $1 \mu\text{m}$ ) was selected to remove larger undissolved aggregates. Only smaller Sepia particles were therefore probed akin to the smaller particles resolved in the study by Nofsinger *et al.*<sup>16</sup> The sample synthesis and preparation details are given in the supplementary material.<sup>13</sup> We characterized both melanin samples with UV-visible absorption spectroscopy and 1 mm spectrophotometer cuvettes (Starna cells) were used for all transient absorption measurements. Both spectra can be fit reasonably well

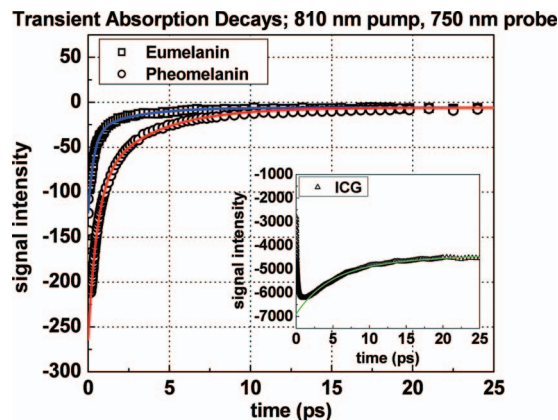


FIG. 2. Transient absorption decays and fits for Sepia eumelanin and synthetic pheomelanin. Convention: negative signal implies ground state depletion. The decays were normalized for laser intensity and pump absorbance. The inset graph shows the transient absorption of an ICG calibration sample which was used to determine melanin molar absorptivities by correlating the extrapolated lock-in signal intensity at time zero with the known molar absorptivity of ICG.

using an exponential function (with a decay constant  $k_m$  normalized at 400 nm) over the range of 350–900 nm. We obtained  $k_m$  values of 2.1 and 3.6 for the Sepia eumelanin and synthetic pheomelanin solutions which lie in the range of values measured for these types of samples.<sup>8</sup>

Figure 2 displays transient absorption decays for eumelanin and pheomelanin when pumping and probing at 810 and 750 nm, respectively. Both decays exhibit a negative signal, which is attributed to ground state depletion. Stimulated emission and fluorescence signals are negligible when probing at higher energy because excited state relaxations dictate that emission will occur at longer wavelengths. Any bleed through of fluorescence will also be minimal because of melanin's low fluorescence quantum yield<sup>17</sup> and would only give rise to a signal offset since we do not time resolve fluorescent photons. Figure 2 displays that signal offsets contribute  $<1\%$  at long interpulse delays and therefore fluorescence is not considered further. Excited state absorption may occur, although at these wavelengths it is dominated by ground state depletion since the signals are negative. We consider the effects of excited state absorption in the analysis given below. Blanchard and Wirth<sup>18</sup> have shown that under such circumstances and low sample absorbance, the transient absorption signal has the following dependence (by extension to  $N$  species with overlapping spectra and without excited state population decay),

$$\Delta I_{\text{pr}}(\lambda_{\text{pu}}, \lambda_{\text{pr}}) \propto I(\lambda_{\text{pu}})I(\lambda_{\text{pr}})b \sum_{i=1}^N C_i \varepsilon_i(\lambda_{\text{pu}}) \varepsilon_i(\lambda_{\text{pr}}). \quad (1)$$

The change in probe intensity  $[\Delta I_{\text{pr}}(\lambda_{\text{pu}}, \lambda_{\text{pr}})]$  is proportional to the intensities of the pump and probe pulses  $[I(\lambda_{\text{pu}}), I(\lambda_{\text{pr}})]$ , the path length ( $b$ ), the concentrations of each species ( $C_i$ ) and the molar absorptivities of each species at the pump and probe wavelengths  $[\varepsilon_i(\lambda_{\text{pu}}), \varepsilon_i(\lambda_{\text{pr}})]$ . Equation (1) accounts for the fact that melanins likely consist of more than one dominant molecular species since different precursors may polymerize in various ways to form the

TABLE I. Linear and nonlinear absorption parameters for melanins measured at 750 nm. Bold/italicized entries were determined by calculations using the calibrated laser spectrometer values from the ICG solution and the Beer–Lambert law

Sample	T.A. Signal ( $\mu\text{V}$ )	Absorbance (O.D.)	Molar absorptivity ( $\text{M}^{-1}\text{cm}^{-1}$ )	Concentration ( $\mu\text{M}$ )	Molar mass (g/mol)	Monomers
Indocyanine green	-6890	0.033	<b>82 500</b>	4	775	1
Sepia eumelanin	-120	0.014	<b>1500</b>	92	<b>9130</b>	53 <sup>a</sup>
Synthetic pheomelanin	-262	0.036	<b>3200</b>	<b>111</b>	<b>7570</b>	28

<sup>a</sup>Note that the entry does not take into account the mass of proteins, metals, and lipids found in Sepia granules (see text).

pigments.<sup>17,19,20</sup> Equation (1) may be further simplified to yield,

$$\Delta I_{\text{pr}}(\lambda_{\text{pu}}, \lambda_{\text{pr}}) \approx I(\lambda_{\text{pu}})I(\lambda_{\text{pr}})bC_{\text{total}}\bar{\epsilon}(\lambda_{\text{pu}})\bar{\epsilon}(\lambda_{\text{pr}}). \quad (2)$$

The mean molar absorptivities [ $\bar{\epsilon}(\lambda_{\text{pu}})$ ,  $\bar{\epsilon}(\lambda_{\text{pr}})$ ] were factored out of the summation in Eq. (1) resulting in a summation over concentrations ( $C_{\text{total}}$ -molar concentration of all pigments). This approximation is reasonable for melanins provided that all constituent pigments exhibit broad overlapping absorption spectra as opposed to distinct nonoverlapping bands for each species. Recent calculations have verified this for a variety of eumelanin oligomers and more extended polymers.<sup>8,21</sup> The absorption spectra of some pheomelanin precursors also exhibit this feature.<sup>20</sup> Equation (2) illustrates that when the transient absorption signal is normalized for the laser intensities and absorbance at the pump wavelength (Fig. 2), the signal is proportional to the mean molar absorptivity at the probe wavelength [ $\bar{\epsilon}(\lambda_{\text{pr}})$ ]. In order to determine the absolute value of  $\bar{\epsilon}(\lambda_{\text{pr}})$  for the melanins, the spectrometer was calibrated using a 4  $\mu\text{M}$  solution of Indocyanine green (ICG or IR 125; Exciton) dissolved in methanol (1 mm cuvette). It serves as an ideal standard solution because ICG's optical properties are well characterized<sup>22</sup> and it also exhibits a dominant ground state depletion signal (Fig. 2 inset). While fluorescence does occur in ICG, its effect is also minimal for the same reason stated above for melanins. Fluorescent photons would give rise to a flat signal offset at all times because we do not time resolve fluorescence and its occurrence does not depend on the arrival of the probe pulse. The inset in Fig. 2 shows the negligible signal intensities before time zero for ICG. Excited state (sequential two-photon) absorption of ICG is also negligible because it does not have an appreciable single photon transition at  $\sim\lambda_{\text{exc}}/2 \approx 400$  nm, which is typically observed in organic molecules exhibiting multiphoton absorptions.<sup>23</sup> By extrapolating all signals to time zero (before excited state relaxation takes place) we correlate signal intensity on the lock-in amplifier with the known molar absorptivity for ICG and consequently determine it for eumelanin and pheomelanin via a ratiometric approach.

The early time signals in Fig. 2 illustrate that pheomelanin absorbs more strongly than eumelanin at 750 nm (3200 versus 1500  $\text{M}^{-1}\text{cm}^{-1}$  after calibration—see Table I above). Under the approximation used in Eq. (2), we can construct an average molar absorptivity spectrum for eumelanin and pheomelanin by extrapolating the shape of the linear absorp-

tion spectrum to shorter wavelengths. As indicated above for melanins, the shape of the absorption spectrum is dominated by wavelength dependent molar absorptivities and not a concentration distribution of species absorbing at distinct wavelengths. For this reason, Fig. 3 was constructed to display the mean molar absorptivity spectra for eumelanin and pheomelanin. Because pheomelanin exhibits a steeper absorption slope relative to eumelanin, it absorbs more strongly over the entire spectral range; in particular at UV wavelengths. The data imply that less quantities of pheomelanin relative to eumelanin are required to absorb UV photons. This is intriguing considering that UV radiation has been shown to initiate detrimental photochemical processes involving pheomelanin.<sup>24</sup>

The molar absorptivities of eumelanin and pheomelanin may be used to extract an average molecular weight for the pigments by the application of the Beer–Lambert law. Scattering contributions to the absorption spectrum are ignored as Riesz *et al.*<sup>25</sup> (and references therein) have shown their contributions to be small ( $<6\%$ ) at UV wavelengths and are therefore negligible at near IR wavelengths where scattering is significantly smaller. First of all, the molar concentrations of eumelanin and pheomelanin are readily calculated from the absorption spectra because the absorbances, molar absorptivities and path length are known. Since the mass and molar concentrations are known, the average molar mass for each pigment may be estimated (mass concentration/molar concentration) and the values are given in Table I. Given that the estimated average monomer molar mass is 171 g/mol for eumelanin (indoles) and 274 g/mol for pheomelanin (benzothiazines),<sup>19</sup> as shown in Fig. 1, and that Sepia gran-

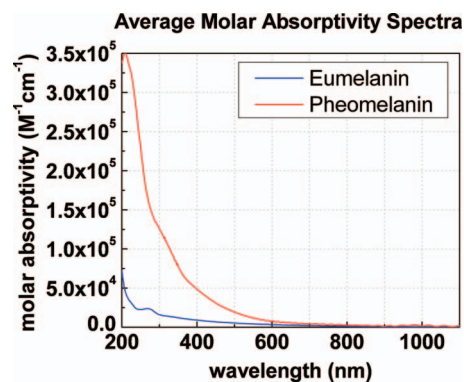


FIG. 3. Average molar absorptivity spectra for pigments in Sepia eumelanin and synthetic pheomelanin.

ules typically contain ~5% of proteins,<sup>14</sup> 5% of metals,<sup>26</sup> and <4% of lipids by weight<sup>27</sup> (~14% total non pigment mass), we determine that the average pigment size consists of ~46 and 28 monomer units respectively. Table I summarizes the calibration and calculated values. These values would be even greater for melanins in the presence of excited state absorption since the effective ground state depletion signals shown in Fig. 2 would be larger. This is significantly larger than the melanin oligomers that have been postulated to give rise to the optical properties of eumelanin. The data emphasize that pigments of larger sizes exist and may therefore give rise to more delocalized properties.

In summary, some important optical and structural features have been deduced for model melanin systems. Synthetic pheomelanin has a greater molar absorptivity than Sepia eumelanin over a large spectral range (UV-near IR). The molar absorptivities were used to estimate the average size of melanin polymers revealing that these pigments consist of structures containing tens of monomers. This is in contrast with recent structural models that have suggested that small oligomers (four to six units) represent the fundamental unit of eumelanin. If these oligomers do exist in eumelanin, then coupling of interoligomer layers via covalent bonding may account for the larger pigment sizes observed in this study. Further nonlinear optical studies will shed light on the extent of delocalized excitations in a wider variety of synthetic and natural melanin samples over a broader spectral range.

<sup>1</sup>J. B. Nofsinger, T. Ye, and J. D. Simon, *J. Phys. Chem. B* **105**, 2864 (2001).

<sup>2</sup>S. Ito and K. Fujita, *Anal. Biochem.* **144**, 527 (1985).

<sup>3</sup>K. Wakamatsu and S. Ito, *Pigment Cell Res.* **15**, 174 (2002).

<sup>4</sup>J. Cheng, S. C. Moss, and M. Eisner, *Pigment Cell Res.* **7**, 263 (1994); G. W. Zajac, J. M. Gallas, J. Cheng, M. Eisner, S. C. Moss, and A. E.

Alvaradoswaisgood, *Biochim. Biophys. Acta* **1199**, 271 (1994).

<sup>5</sup>Y. Liu and J. D. Simon, *Pigment Cell Res.* **16**, 606 (2003).

<sup>6</sup>A. Pullman and B. Pullman, *Biochim. Biophys. Acta* **54**, 384 (1961).

<sup>7</sup>M. L. Tran, B. J. Powell, and P. Meredith, *Biophys. J.* **90**, 743 (2006).

<sup>8</sup>G. Zonios, A. Dimou, I. Bassukas, D. Galaris, A. Tsolakidis, and E. Kaxiras, *J. Biomed. Opt.* **13**, 014017 (2008).

<sup>9</sup>J. McGinness, P. Corry, and P. Proctor, *Science* **183**, 853 (1974).

<sup>10</sup>T. Ye and J. D. Simon, *J. Phys. Chem. B* **107**, 11240 (2003).

<sup>11</sup>A. Orstan and J. B. A. Ross, *J. Phys. Chem.* **91**, 2739 (1987); A. Napolitano, P. Di Donato, G. Protta, and E. J. Land, *Free Radic Biol. Med.* **27**, 521 (1999).

<sup>12</sup>D. Fu, T. E. Matthews, I. R. Piletic, and W. S. Warren, *J. Biomed. Opt.* **13**, 0405031 (2008); D. Fu, T. Ye, T. E. Matthews, J. Grichnik, L. Hong, J. D. Simon, and W. S. Warren, *J. Biomed. Opt.* **13**, 054036 (2008).

<sup>13</sup>See EPAPS supplementary material at <http://dx.doi.org/10.1063/1.3265861> for a description of the laser apparatus and sample preparation.

<sup>14</sup>Y. Liu, L. Hong, K. Wakamatsu, S. Ito, B. Adhyaru, C. Y. Cheng, C. R. Bowers, and J. D. Simon, *Photochem. Photobiol.* **81**, 135 (2005).

<sup>15</sup>S. Ito, *Pigment Cell Res.* **2**, 53 (1989).

<sup>16</sup>J. B. Nofsinger, S. E. Forest, and J. D. Simon, *J. Phys. Chem. B* **103**, 11428 (1999).

<sup>17</sup>P. Meredith, B. J. Powell, J. Riesz, S. P. Nighswander-Rempel, M. R. Pederson, and E. G. Moore, *Soft Matter* **2**, 37 (2006).

<sup>18</sup>G. J. Blanchard and M. J. Wirth, *Anal. Chem.* **58**, 532 (1986).

<sup>19</sup>S. Ito and K. Wakamatsu, *Pigment Cell Res.* **16**, 523 (2003).

<sup>20</sup>A. Napolitano, M. De Lucia, L. Panzella, and M. d'Ischia, *Photochem. Photobiol.* **84**, 593 (2008).

<sup>21</sup>E. Kaxiras, A. Tsolakidis, G. Zonios, and S. Meng, *Phys. Rev. Lett.* **97**, 218102 (2006); S. Meng and E. Kaxiras, *Biophys. J.* **94**, 2095 (2008).

<sup>22</sup>R. Philip, A. Penzkofer, W. Baumler, R. M. Szeimies, and C. Abels, *J. Photochem. Photobiol., A* **96**, 137 (1996).

<sup>23</sup>M. Albota, D. Beljonne, J. L. Bredas, J. E. Ehrlich, J. Y. Fu, A. A. Heikal, S. E. Hess, T. Kogej, M. D. Levin, S. R. Marder, D. McCord-Maughon, J. W. Perry, H. Rockel, M. Rumi, C. Subramaniam, W. W. Webb, X. L. Wu, and C. Xu, *Science* **281**, 1653 (1998).

<sup>24</sup>T. Ye, L. Hong, J. Garguilo, A. Pawlak, G. S. Edwards, R. J. Nemanich, T. Sarna, and J. D. Simon, *Photochem. Photobiol.* **82**, 733 (2006).

<sup>25</sup>J. Riesz, J. Gilmore, and P. Meredith, *Biophys. J.* **90**, 4137 (2006).

<sup>26</sup>Y. Liu and J. D. Simon, *Pigment Cell Res.* **18**, 42 (2005).

<sup>27</sup>E. Vedralova and J. Duchon, *Neoplasma* **30**, 317 (1983).